

Chapter 6

Power Amplifiers

In this chapter, power amplifiers for synchrotron and storage ring RF systems are discussed. The main task of the power amplifier is to provide RF power to the synchrotron cavity. This is done by conversion from DC to RF power. The DC power is drawn from the line power by means of power supplies that are responsible for providing all voltages and currents that are required to operate the power amplifier.

A variety of devices are used in power amplifiers for particle accelerators [1,2]:

- **Gridded vacuum tubes** (e.g., triodes, tetrodes) [3,4]
- **Inductive output tubes, IOTs** (klystrode) [5]
- **Klystrons** [6]
- **Solid state amplifiers**

The first three types (gridded tubes, inductive output tubes, and klystrons) are **vacuum tubes**. These devices thermionically liberate electrons from a cathode to create a high-current electron beam, which is accelerated by a high DC voltage toward the anode (collector). The beam always travels within a vacuum to reduce interaction with rest gas. After emission, the beam is bunched. If gridded tubes and inductive output tubes are used, this bunching is done by a fine grid in front of the cathode. The voltage of this grid is modulated with the desired frequency, thereby directly modulating the current through the tube. In a klystron, this bunching is done by modulating the voltage in one or typically several buncher cavities, thereby bunching the coasting beam emitted from the gun in flight.

For gridded tubes, the voltage of the anode is modulated by the impacting beam, and the RF current is directly drawn from there. If an inductive output tube and klystron are used, then the modulated electron beam travels through a catcher cavity in front of the collector, where it excites an electromagnetic field. The power from this catcher cavity is extracted by a coupler and can be delivered to the load.

Solid-state amplifiers consist of a large number of transistors operating in parallel. Due to the reduced mobility of the electrons within the transistor compared to vacuum, the output power of solid-state amplifiers at high frequencies is rather

This chapter has been made open access under a CC BY-NC-ND 4.0 license. For details on rights and licenses please read the Correction https://doi.org/10.1007/978-3-319-07188-6_8

limited compared to vacuum tubes, usually restricting them to medium power applications such as driver amplifiers (even though their range of application is being extended continually).

The three different types of vacuum tubes are used in different applications with respect to particle accelerators. The factors that are most important in determining the choice are the operating frequency of the power amplifier and whether it is a narrowband or a broadband application. Generally, gridded tubes are favorable at frequencies below a few hundred megahertz. At high frequencies, gridded tubes are limited by time-of-flight effects. Tubes usually have a high bandwidth, since they do not exhibit any low-frequency limitations. Klystrons, on the other hand, are unsuited for low-frequency operation, since their dimensions become impractical in this case. In addition, the frequency band of klystrons is rather limited, due to the bandwidth of the cavities it uses. Inductive output tubes fall between the operating frequencies of gridded tubes and klystrons. Summarizing, gridded tubes are favorable in applications below 100 MHz, especially if broadband behavior is required. Klystrons are optimal for high-frequency narrowband applications. In general, hadron synchrotron and storage ring RF systems fall in the former category (low frequency, broadband), and therefore gridded vacuum tubes are usually the best choice for a power amplifier for this type of RF system. Tubes are also much less sensitive than semiconductors to a high radiation dose environment. Therefore, the following section will focus on power amplifiers using gridded vacuum tubes.

6.1 Gridded Vacuum Tubes

In this section, different types of gridded vacuum tubes are discussed. More detailed information may be found, for example, in [3], which also influenced the presentation in this book.

6.1.1 Diode

The simplest type of vacuum tube is a **diode**, as shown in Fig. 6.1. A vacuum diode features two **electrodes**: a **cathode** and an **anode** (also called **plate**) in a vacuum environment. A cylindrical arrangement with an outer anode cylinder enclosing an inner cathode cylinder is usually used. This assembly is enclosed in a compartment made of metal or glass with several feedthroughs to connect the electrodes. The cathode is heated by means of an electric current to initiate the **thermionic emission** of electrons, thereby introducing free charge carriers into the vacuum. When one now applies a positive voltage to the anode with respect to the cathode, these electrons may travel through the diode, creating a negative current flowing from the cathode to the anode.

Fig. 6.1 Schematic view of a diode

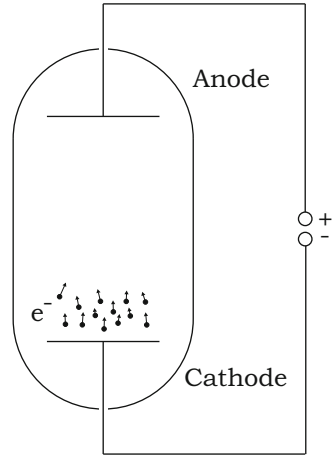
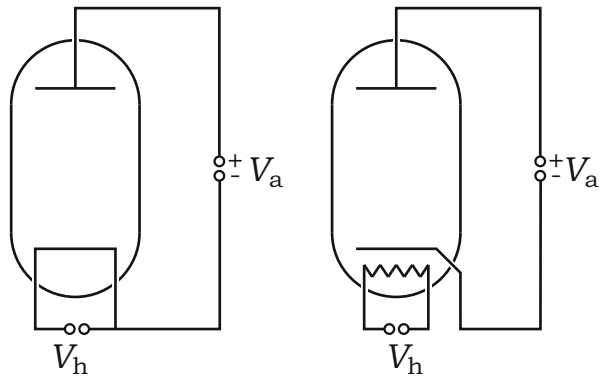


Fig. 6.2 Directly heated cathode (*left diagram*) and indirectly heated cathode (*right diagram*)



As we will see later, this current is dependent on the type of vacuum tube (geometry, material selection), the temperature of the cathode, the vacuum pressure, and the voltage between anode and cathode.

Reversing the polarity of both electrodes results in no current flowing through the device, since the anode is not heated. No electrons will be emitted from the anode that can travel through the tube. On the other hand, all electrons emitted from the cathode will also not be able to pass through the tube, due to the voltage barrier introduced by the anode. The transport of (negative) current through a vacuum tube is possible from only the cathode to the anode. Therefore, a vacuum diode may be used for rectification purposes, similar to semiconductor diodes.

The heating of the cathode can be done in two different ways. For **direct heating**, as shown in the left-hand diagram of Fig. 6.2, the current used to increase the temperature of the cathode travels directly through the cathode. For **indirect heating** (see the right-hand diagram of Fig. 6.2), a dedicated **filament** allows the heating of the cathode. In addition to this, the heating may be performed by DC or AC.

A directly heated cathode with one side of the cathode at ground potential and the other side at the heating potential exhibits a voltage drop over its length. This voltage

drop leads to different voltages between different parts of the cathode and the anode, thereby influencing the current traveling through the tube. To reduce this effect, as well as the self-heating of the cathode by the emitted electrons, the resistance of the cathode is usually chosen to be fairly low. Nevertheless, in case of AC heating, a modulation of the tube current with the frequency of the heating current (usually 50 Hz) is observed, and a correction may be necessary, depending on the application. In an indirect heating scheme, the whole cathode remains at an almost constant potential. In addition to this, the total area of an indirectly heated cathode is usually much larger than that of the wire configuration of a directly heated one. AC heating without any corrections is applied whenever possible. On the other hand, the required heating power is much larger than in the direct heating scheme, due to the larger volume that is kept at high temperature. Especially for high-power tubes, this may become a limiting factor. It will also take much longer for an indirectly heated cathode to reach its operating temperature. The temperature and therefore the current density that can be emitted from an indirectly heated cathode is smaller than that of a directly heated one.

In the following, the current density emitted by such a heated cathode will be discussed. Electrons within the cathode are bound to the metal. To release them into the vacuum, they have to overcome the binding energy of the metal (electron work function), which is usually on the order of a few electron volts. The electrons inside the metal exhibit different energies; they follow a band structure with a partly occupied conduction band.

The emitted current density is calculated assuming an infinite plane surface. The emission takes place perpendicular to this surface, along the z -axis.

The density of states n_{stat} inside the metal is given by

$$dn_{\text{stat}} = 4\pi \left(\frac{2m_e}{h^2} \right)^{3/2} \sqrt{W} dW,$$

with the electron mass m_e , **Planck's constant** h , and the energy W of the observed state. The density of occupied states dn is given as the product of the density of states dn_{stat} and the distribution function $F(W)$ obeying the **Fermi-Dirac statistics**

$$F(W) = \frac{1}{1 + e^{\frac{W - W_F}{k_B T}}} \approx e^{-\frac{W_F - W}{k_B T}}, \quad (6.1)$$

where W_F is the **Fermi energy**, $k_B = 8.6173 \cdot 10^{-5}$ eV/K **Boltzmann's constant**, and T the (absolute) temperature. One can see that at $T = 0$ K, the energy distribution of the electrons has a sharp edge (at the Fermi energy) with all lower states occupied and all states above empty. Once the temperature increases, higher-energy states inside the band structure of the metal and even unbound states begin to become populated. Here, we are interested in electrons featuring these unbound states, because they represent electrons that are thermionically emitted from the cathode. Taking tungsten as an example, the temperature must be below the melting point 3695 K. Therefore, $k_B T$ is below 0.318 eV, which is much smaller than the

binding energy $W_{\text{bind}} = 4.5 \text{ eV}$. This explains the approximation in the last step, since we are interested in unbound states where $W - W_{\text{F}}$ is sufficiently large in comparison with $k_{\text{B}}T$.

The product of the last two equations yields

$$dn = F(W) dn_{\text{stat}} = 4\pi \left(\frac{2m_{\text{e}}}{h^2} \right)^{3/2} e^{\frac{W_{\text{F}} - W}{k_{\text{B}}T}} \sqrt{W} dW.$$

The calculation is simpler when we are discussing the momentum p instead of the energy $W = \frac{p^2}{2m_{\text{e}}}$:

$$dn = \frac{8\pi}{h^3} e^{\frac{W_{\text{F}} - \frac{p^2}{2m_{\text{e}}}}{k_{\text{B}}T}} p^2 dp.$$

We will now use the formula

$$4\pi p^2 dp = dp_x dp_y dp_z,$$

where dp_x , dp_y , and dp_z are the differentials of the momentum components in Cartesian coordinates. Furthermore, due to

$$\vec{J} = \rho_q \vec{v},$$

the differential of the current density in the z -direction is given by

$$dJ_z = -ev_z dn = -e \frac{p_z}{m_{\text{e}}} dn.$$

This results in¹

$$dJ_z = -\frac{2e}{h^3 m_{\text{e}}} e^{\frac{W_{\text{F}} - \frac{p^2}{2m_{\text{e}}}}{k_{\text{B}}T}} p_z dp_x dp_y dp_z.$$

Integrating this equation in the x - and y -directions from minus infinity to infinity and in the z -direction from p_{vac} to infinity accounts only for such electrons with sufficient energy to be able to leave the metal, thereby forming a current density J_z in the z -direction:

$$J_z = -\frac{2e}{h^3 m_{\text{e}}} e^{\frac{W_{\text{F}}}{k_{\text{B}}T}} \int_{-\infty}^{\infty} e^{-\frac{p_x^2}{2m_{\text{e}}k_{\text{B}}T}} dp_x \int_{-\infty}^{\infty} e^{-\frac{p_y^2}{2m_{\text{e}}k_{\text{B}}T}} dp_y \int_{p_{\text{vac}}}^{\infty} e^{-\frac{p_z^2}{2m_{\text{e}}k_{\text{B}}T}} p_z dp_z.$$

¹Please note that in this equation and in the following, the same symbol e is used for the elementary charge and Euler's constant. Since the latter is the base of the exponential function, this should not lead to misunderstanding.

The first two integrals are of the type

$$\int_{-\infty}^{\infty} e^{-ax^2} dx = \sqrt{\frac{\pi}{a}} \quad (a > 0),$$

and the third integral is

$$\int x e^{-ax^2} dx = -\frac{e^{-ax^2}}{2a} + \text{const.}$$

This leads to

$$J_z = -\frac{4\pi e k_B T}{h^3} e^{\frac{W_F}{k_B T}} m_e k_B T e^{-\frac{p_{\text{vac}}^2}{2m_e k_B T}}.$$

Substituting the momentum again for the energy and observing² that

$$W_{\text{bind}} = W_{\text{vac}} - W_F$$

yields the **Richardson or Richardson–Dushman equation**

$$J_S = -J_z = A_R T^2 e^{-\frac{W_{\text{bind}}}{k_B T}} \quad (6.2)$$

with the **Richardson constant**

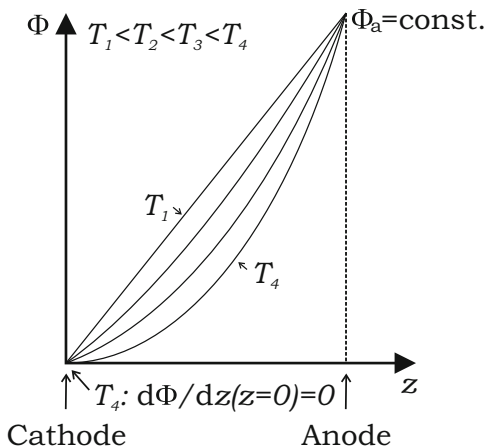
$$A_R = \frac{4\pi m_e k_B^2 e}{h^3} \approx 120 \frac{\text{A}}{\text{cm}^2 \text{K}^2}.$$

For the operation of a vacuum tube, a high-saturation current density J_S is desirable. Therefore, the cathode is operated at high temperature, and the cathode material is chosen so as to exhibit a low binding energy and the ability to withstand operation at these high temperatures. For high-power applications, tungsten or thoriated tungsten is usually employed.

In applying an electric field at the surface of the metal, the binding energy is slightly reduced. This leads to an increase in emission from the cathode. This phenomenon is called the **Schottky effect**. The reduction in binding energy amounts to

² p_{vac} is the momentum corresponding to the energy W_{vac} , which denotes the potential energy of an electron in vacuum just outside of the metal; W_{bind} is the binding energy, which denotes the minimal energy (at $T = 0$) required to remove an electron from the metal. For metals, this quantity is equal to the work function, which at $T = 0$, denotes the energy required to transfer an electron from Fermi energy to the outside of the metal (vacuum energy). Usually, all energies are referenced relative to $W_{\text{vac}} = 0$.

Fig. 6.3 Evolution of an idealized potential distribution between cathode and anode with increasing temperature (increasing charge density)

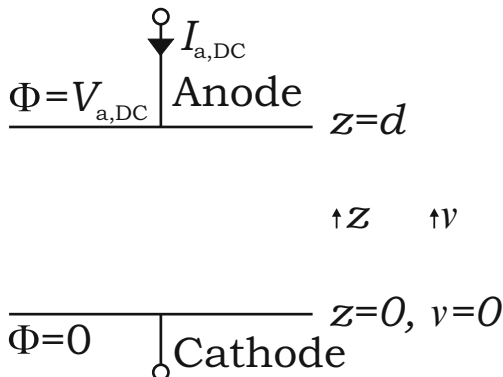


$$\Delta W = \sqrt{\frac{e^3 E_{\text{surf}}}{4\pi\epsilon_0}}, \tag{6.3}$$

with E_{surf} the electric field strength at the surface of the cathode.

Under some circumstances, not all of the electrons that are emitted by the cathode can travel to the anode. The potential distribution between the cathode and the anode is defined not only by the potential difference and the geometric arrangement between these electrodes. The electrons that are traveling from the cathode to the anode also influence the potential distribution due to the charge they are introducing. This effect is called **space charge**. Under some operational conditions, the presence of these electrons can constitute a limiting factor with respect to the total current that can travel through the tube. To illustrate this effect, consider two parallel electrodes. Without any space charge effects, the potential distribution between these electrodes is given by the straight line shown in Fig. 6.3 denoted by T_1 (no heating). If we now begin to heat the cathode, electrons are emitted, and all of them travel from the cathode to the anode, thereby introducing charge carriers in the space between the electrodes. These charge carriers will now begin to have an influence on the potential, as shown by the curve T_2 in Fig. 6.3. They will shield the potential seen from the anode. This effect is most pronounced at the cathode. When one increases the temperature of the cathode, the number of electrons that are emitted increases according to Eq. (6.2). All these electrons will travel to the anode, thereby further amplifying the space charge effects and flattening out the potential distribution. These mechanisms continue with rising temperature (T_2, T_3) until the gradient of the modified potential at the location of the cathode becomes zero ($\text{grad } \Phi = -\vec{E} = 0$) at temperature T_4 . The electric field at the location of the cathode now vanishes. And with rising temperature, any additional electrons that are emitted by the cathode will be unable to travel from the cathode to the anode. An electron cloud is formed at the cathode, where electrons emitted from the cathode are in equilibrium with

Fig. 6.4 Arrangement of two parallel electrodes used to derive the space charge limited current



electrons that move from the cloud back into the cathode. So from the temperature T_4 upward, the current transported through the tube is almost independent of the cathode temperature; the potential distribution also remains unchanged.

Let us now calculate this effect under the following conditions (see Fig. 6.4):

- Two infinitely extended plane electrodes that are separated in the z -direction by d with constant potentials:

$$\Phi|_{z=0} = 0, \quad \Phi|_{z=d} = V_{a,DC} \quad (\text{Dirichlet boundary condition}).$$

- The current density is limited by space charge effects:

$$\left. \frac{d\Phi}{dz} \right|_{z=0} = 0.$$

- The electrons are the only charge carriers between the electrodes.
- The electrons are emitted with zero velocity:

$$v|_{z=0} = 0.$$

- The electron energies are sufficiently small; relativistic effects are negligible.
- The change in anode voltage is slow compared to the transit time of the electrons.
- All magnetic fields in the diode caused by the moving electrons in the vacuum as well as in the conductors (e.g., cathode) are neglected.

The distribution of the potential is given by the Poisson equation (2.54),

$$\Delta \Phi = -\frac{\rho_q}{\epsilon_0}, \tag{6.4}$$

where Φ is the electric potential and ρ_q the space charge density.

Calculating the potential for two plate electrodes of infinite dimensions that are separated in the z -direction leads to

$$\frac{d^2\Phi}{dz^2} = -\frac{\rho_q}{\epsilon_0}. \quad (6.5)$$

The charge and the current density are connected by the relation

$$J = -J_z = -\rho_q v, \quad (6.6)$$

where v is the velocity of the electrons.

The kinetic energy of the electrons (nonrelativistic case)³ is equal to the electric energy gain:

$$\Phi e = \frac{1}{2} m_e v^2. \quad (6.7)$$

Here m_e denotes the mass of the electrons. Combining the last three equations yields

$$\frac{d^2\Phi}{dz^2} = kJ\Phi^{-1/2}, \quad (6.8)$$

with

$$k = \frac{1}{\epsilon_0} \sqrt{\frac{m_e}{2e}}$$

constant. It follows that

$$\begin{aligned} 2 \frac{d\Phi}{dz} \frac{d^2\Phi}{dz^2} &= 2kJ\Phi^{-1/2} \frac{d\Phi}{dz} \\ \Rightarrow \frac{d}{dz} \left[\left(\frac{d\Phi}{dz} \right)^2 \right] &= 2kJ\Phi^{-1/2} \frac{d\Phi}{dz}. \end{aligned}$$

The current density J remains constant with varying z . By means of an integration, we obtain

$$\begin{aligned} \left(\frac{d\Phi}{dz} \right)^2 &= 2kJ \int \Phi^{-1/2} \frac{d\Phi}{dz} dz \\ \Rightarrow \left(\frac{d\Phi}{dz} \right)^2 &= 4kJ\Phi^{+1/2} + A. \end{aligned}$$

³The following example illustrates this assumption: for electrons with a kinetic energy of 20 keV one gets

$$\beta = 0.2719, \quad \gamma = 1.03914,$$

and the error of the nonrelativistic formula for the kinetic energy is about 5.9%.

At the surface of the cathode,

$$\Phi|_{z=0} = 0, \quad \left. \frac{d\Phi}{dz} \right|_{z=0} = 0$$

is valid. This results in $A = 0$, and we obtain

$$\begin{aligned} \frac{d\Phi}{dz} &= 2\sqrt{kJ}\Phi^{1/4} \\ \Rightarrow \int \Phi^{-1/4} d\Phi &= 2\sqrt{kJ} \int dz \\ \Rightarrow \frac{4}{3}\Phi^{3/4} &= 2\sqrt{kJ}z + B. \end{aligned}$$

Using the boundary condition

$$\Phi|_{z=0} = 0$$

at the cathode and

$$\Phi|_{z=d} = V_{a,DC}$$

results in $B = 0$ and

$$\begin{aligned} \frac{2}{3}V_{a,DC}^{3/4} &= \sqrt{kJ}d \\ \Rightarrow V_{a,DC} &= \left(\frac{3}{2}d\sqrt{k}\right)^{4/3} J^{2/3}. \end{aligned}$$

This equation gives the dependency of the potential in the space-charge-limited case. The line depicting T_4 in Fig. 6.3 follows this $d^{4/3}$ dependency. Regarding the current density, we have

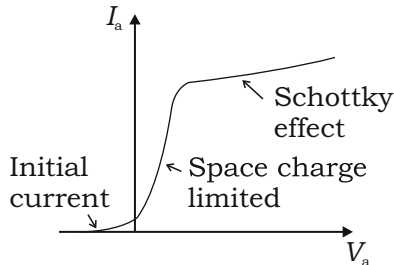
$$J = \frac{4}{9kd^2} V_{a,DC}^{3/2}, \quad (6.9)$$

or in general, for different geometric conditions and integrating over the whole cathode surface A_c , we have

$$I_{a,DC} = KA_c V_{a,DC}^{3/2},$$

with $I_{a,DC}$ the total current traveling through the tube. If we assume that the voltage and the current will change slowly enough to justify our static field calculation, we may use this equation also in the non-DC case:

Fig. 6.5 Characteristic current curve of a vacuum diode; the axes are not true to scale



$$I_a = KA_c V_a^{3/2}. \tag{6.10}$$

This equation is called **Child’s law or the Langmuir–Child law**, stating that the current is proportional to the power of 3/2 of the voltage between both electrodes. The constant K depends on the geometry of the tube. For the planar electrodes considered so far, we get

$$K = \frac{4}{9kd^2} = \frac{4\epsilon_0}{9d^2} \sqrt{\frac{2e}{m_e}}.$$

A more detailed analysis of the behavior of electrons between two parallel electrodes under space charge conditions, which also takes different initial velocities into account, is given in [7].

For tubes, a cylindrical assembly of a cathode with an outer radius r_c and an anode with an inner radius of r_a is often realized ($r_a > r_c$). This configuration yields, for a long cylinder [8],

$$K = \frac{4\epsilon_0}{9r_c^2} \sqrt{\frac{2e}{m_e}} \left(\frac{r_a}{r_c} - 1\right)^{-1/2} \left(\ln \frac{r_a}{r_c}\right)^{-3/2}. \tag{6.11}$$

Figure 6.5 shows a typical characteristic curve of a vacuum diode. Plotted here is the current through the diode as a function of the voltage between cathode and anode at a constant cathode temperature.

One can distinguish three different sections. The first part, where the anode voltage is negative, is called area of initial current. Here the current rises exponentially with the voltage. This behavior can be described by Eq. (6.2) modified in that the electrons now have to overcome not only the binding energy of the metal but also the potential difference between both electrodes:

$$J = A_R T^2 e^{-\frac{W_{\text{bind}} - eV_{a,\text{DC}}}{k_B T}}. \tag{6.12}$$

This equation is valid as long as the current is not limited by space charge effects, which will become relevant even at negative anode voltages. Only the electrons that

leave the metal with sufficient kinetic energy are capable of doing so; therefore, the current is strongly dependent on the temperature of the cathode. In general, the magnitude of this initial current is much lower (several orders of magnitude) than that of the saturation current. With increasing anode voltage, the behavior of the anode current is dominated by space charge effects; it is almost independent of the cathode temperature; its devolution with the anode voltage is given by Eq. (6.10). This behavior remains intact with increasing anode voltage until the current reaches the saturation current given by Eq. (6.2). At that point, all electrons that are emitted from the cathode can travel through the diode; space charge effects are no longer relevant with respect to the current. The current will again become dominated by the temperature of the cathode. This transition is not sharp, since the temperature is not constant over the whole cathode. When one continues to raise the voltage, the saturation current increases slowly according to the Schottky effect; see Eq. (6.3).

In the scope of this chapter, vacuum tubes will be applied in amplifiers. Here, one wants the current of the tube to be strongly influenced by the anode or grid voltage. In addition, it is beneficial if the current does not depend on the temperature of the cathode, allowing much more relaxed requirements regarding temperature stability. Therefore, vacuum tubes in amplifier configuration are generally operated in the space-charge-dominated region.

6.1.2 Triode

The vacuum diode presented in the previous section is unsuitable for application in an amplifier design, because for a given cathode heating, the tube current is not controllable independently of the anode voltage. To overcome this limitation, an additional cold electrode is introduced into the tube, called the **grid**, resulting in a **triode**. The grid is located between the cathode and the anode; it consists of a metal wire helix or metal mesh with an electrical connection to the outside of the tube. Now, for a given heating current, the electron flux from cathode to anode is a function of the grid and the anode voltage. The following considerations illustrate these dependencies: For a diode, the current in the space-charge-dominated region is given by Eq. (6.10),

$$I_a = \tilde{K}_{\text{diode}} V_a^{3/2},$$

where V_a is given by the capacitance between anode and cathode and the charge induced on the cathode:

$$V_a = \frac{Q_c}{C_{ac}}.$$

In the case of a triode, the current traveling to the anode can be expressed by

$$I_a = \tilde{K}_{\text{triode}} \tilde{V}_{\text{ctrl}}^{3/2}$$

as a function of an effective control voltage

$$\tilde{V}_{\text{ctrl}} = \frac{Q_c}{C_{\text{tot}}}.$$

Here

$$C_{\text{tot}} = C_{\text{ac}} + C_{\text{gc}}$$

represents the combined capacitances of the cathode with respect to the anode and the grid, respectively. The charge Q_c is given by

$$Q_c = C_{\text{ac}} V_a + C_{\text{gc}} V_g,$$

resulting in

$$I_a = \tilde{K}_{\text{triode}} \left(\frac{C_{\text{ac}} V_a + C_{\text{gc}} V_g}{C_{\text{ac}} + C_{\text{gc}}} \right)^{3/2},$$

or

$$I_a = K_{\text{triode}} \left(V_g + \frac{V_a}{\mu_a} \right)^{3/2}. \quad (6.13)$$

Here the behavior of the triode in the space-charge-dominated region is described by means of the amplification factor

$$\mu_a = \frac{C_{\text{gc}}}{C_{\text{ac}}} > 1$$

and

$$K_{\text{triode}} = \tilde{K}_{\text{triode}} \left(\frac{C_{\text{gc}}}{C_{\text{ac}} + C_{\text{gc}}} \right)^{3/2}.$$

The amplification factor μ_a indicates how much stronger the influence of the grid voltage on the anode current turns out to be than that of the anode voltage. The reverse factor $1/\mu_a$ describes the ratio between the influence of a change in the anode voltage on the tube current with respect to a change in the grid voltage.

One can see that a triode can be described as a diode with its anode at the position of the grid whose voltage with respect to the cathode is given by \tilde{V}_{ctrl} . According to Eq. (6.13), three quantities of a triode (I_a , V_g , and V_a) are interconnected. To evaluate the performance of a triode, typically two of these quantities are plotted while one

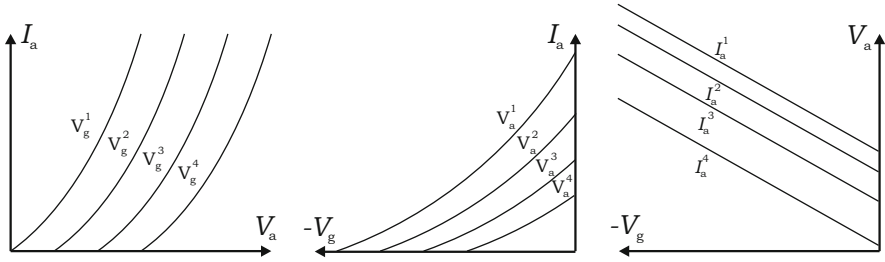


Fig. 6.6 Plate characteristics, mutual characteristics, and constant current curves of a triode

is held constant. If the anode current as a function of the anode voltage is plotted for several constant grid voltages, the plate characteristics are obtained as shown in the first diagram of Fig. 6.6. One can see that for different grid voltages, the curves are shifted with respect to each other along the anode voltage axis, which is due to the different impacts of the grid and anode voltages on the anode current.

The mutual characteristics as shown in the second diagram of Fig. 6.6 display the anode current as a function of the grid voltage for constant anode voltages. Lastly, the constant current curves (right-hand diagram in Fig. 6.6) are obtained if the grid voltage is plotted as a function of the anode voltage for constant anode currents.

In addition to these curves there are three useful quantities to describe the behavior of a triode. These are the amplification factor μ_a mentioned above, the mutual conductance g_m , and the internal resistance R_i . They are given by the following expressions:

$$\mu_a = - \left. \frac{\partial V_a}{\partial V_g} \right|_{I_a = \text{const}}, \quad (6.14)$$

$$g_m = \left. \frac{\partial I_a}{\partial V_g} \right|_{V_a = \text{const}}, \quad (6.15)$$

$$R_i = \left. \frac{\partial V_a}{\partial I_a} \right|_{V_g = \text{const}}. \quad (6.16)$$

The significance of the amplification factor has already been introduced. It can be deduced, for example, from the plate characteristics. The ratio between the shift in anode voltage and the differences in grid voltages between two neighboring constant anode current curves can be used to determine μ_a . The mutual conductance describes the sole impact of a change in grid voltage on the anode current. It is a key figure concerning the amount of amplification that can be realized by a given tube. The mutual conductance can be deduced, for example, by determining the slope of a tangent in the mutual characteristics. Finally, the internal resistance R_i is a measure

of the influence of the anode voltage on the anode current. It is given, for example, by the reciprocal value of the slope of a tangent in the plate characteristic curves.

Based on Eq. (6.13),

$$I_a = K_{\text{triode}} \left(V_g + \frac{V_a}{\mu_a} \right)^{3/2}$$

$$\Leftrightarrow V_a = \mu_a \left[\left(\frac{I_a}{K_{\text{triode}}} \right)^{2/3} - V_g \right],$$

we now calculate the partial derivatives mentioned above. The first result,

$$\frac{\partial V_a}{\partial V_g} = -\mu_a,$$

confirms Eq. (6.14). The other two derivatives are

$$g_m = \frac{\partial I_a}{\partial V_g} = \frac{3}{2} K_{\text{triode}} \left(V_g + \frac{V_a}{\mu_a} \right)^{1/2},$$

$$R_i = \frac{\partial V_a}{\partial I_a} = \frac{2}{3} \mu_a \left(\frac{I_a}{K_{\text{triode}}} \right)^{-1/3} \frac{1}{K_{\text{triode}}} = \frac{2}{3} \mu_a \left(V_g + \frac{V_a}{\mu_a} \right)^{-1/2} \frac{1}{K_{\text{triode}}}.$$

The product of these two equations yields

$$g_m R_i = \mu_a, \quad (6.17)$$

which is often called the **Barkhausen equation**.

6.1.3 Tetrode

In amplifier configurations, especially for RF cavities, **tetrodes** are often employed. Tetrodes exhibit two cold electrodes between the cathode and the anode, the **control grid** (grid 1) and the **screen grid** (grid 2). The main purpose of the control grid is to modulate the anode current, whereas the screen grid is introduced to reduce the reverse amplification factor of the anode. The anode current in the space-charge-limited region is given by

$$I_a = K_{\text{tetrode}} \left(V_{g1} + \frac{V_{g2}}{\mu_{g2}} + \frac{V_a}{\mu_a} \right)^{3/2} \quad (6.18)$$

as a generalization of Eq. (6.13).

6.2 Tube Amplifiers

In this section, RF power amplifiers based on vacuum tubes are discussed. More detailed information may be found, for example, in [9].

In the context of tube amplifiers for synchrotron cavities, the main task of the amplifier is to provide the AC current to achieve the required gap voltages. As discussed in Sect. 4.1.15, the gap voltages used in hadron synchrotron cavities for low harmonic numbers are typically in the range of a few hundred up to a few thousand volts. Since the shunt impedance of these cavities is usually fairly low, at least compared to LINAC cavities or electron synchrotron cavities, the required amplitude of the AC currents is in the range of a few amperes up to dozens of amperes. So in general, the type of amplifier discussed here has to provide high currents at voltage levels of several kilovolts, resulting in power levels of up to several hundreds of kilowatts. In designing an amplifier for this type of application, usually two main goals have to be taken into account: Firstly, the signal quality is an important factor. Every distortion in the current delivered by the tube will lead to a distortion of the gap voltage seen by the beam, albeit reduced by the loaded quality factor of the cavity. These distortions will have an effect on the shape of the bucket. Secondly, the power level of this type of amplifier requires at least some considerations regarding the efficiency of the conversion from DC to AC power. These two requirements contradict each other. In general, an increase in efficiency of a tube amplifier is accompanied by an increase in distortions. So when designing an RF system consisting of amplifier and cavity, a trade-off has to be achieved based on the requirements of this particular system. In classical terms, this type of amplifier can be located somewhere between a broadcast amplifier and a high-power HIFI amplifier. In general, the amplification factor (the ratio between the input and output voltage) is of less concern here, since the input voltage can easily be preamplified to sufficient levels.

Another important topic in designing the power amplifier of a synchrotron RF system is impedance matching. Therefore, it is necessary in most applications to consider the design of the power amplifier and the synchrotron cavity as a combined task. There are many different approaches to achieving this matching, such as by fixing the impedance of the cavity or parts of the cavity that will be driven in parallel to a fixed impedance, usually $50\ \Omega$. In that case, usually one or more semiconductor amplifiers are used. Due to the $50\text{-}\Omega$ regime, it is possible to separate the cavity from the amplifier (e.g., housing the radiation-sensitive semiconductor amplifier in an area separated from the beam line). Another approach regarding the impedance matching is to locate the amplifier very close to the cavity, thereby reducing the length of the power transmission lines as much as possible. In doing so, it is not necessary to match the impedance of the transmission line. We will focus on this scheme, since it allows the transmission of very high power levels from the amplifier to the cavity. In this scheme, again, the impedance of the cavity is a major factor in designing the power amplifier, and it may also be beneficial in designing the cavity

to adapt the impedance seen by the power amplifier in order to allow better matching to certain tubes.

In dealing with this set of requirements, the natural choice of power source is the tetrode. Compared to a triode, the tetrode exhibits a higher amplification factor, due to a screen grid that can be controlled independently of the control grid and the anode voltage. A tetrode can also be operated at lower anode voltages, due to the fact that the control voltage can be kept sufficiently high by a proper choice of the screen grid voltage. This enables a tetrode to be operated in a given scenario at lower DC anode voltages compared to a triode, thereby increasing the efficiency. These benefits generally outweigh the fact that the current emitted by the cathode of a tetrode partly flows to the positive screen grid, reducing the anode current. This effect is fairly small, especially since the geometry of the tetrodes is optimized to minimize it.

Pentodes feature a suppressor grid that prevents secondary electrons emitted by the anode from traveling to the screen grid. In comparing pentodes to tetrodes in the high current operation scheme, this is usually not beneficial, since for the high voltage application discussed here, it is easily achievable to maintain a sufficiently high voltage difference between the anode and the screen grid to block this anode to screen grid current.⁴

Figure 6.7 shows a typical layout of a tetrode-based amplifier in grounded cathode configuration. Here, the cathode of the tube is kept at ground potential. Several voltage supplies are required to operate the tube. A high voltage power supply is responsible for obtaining the voltage difference between cathode and anode. This power supply has to provide fairly high DC currents. In addition, a voltage supply is required to provide the DC voltage of the control grid and another supply will ensure the DC voltage of the screen grid. A filament supply, not shown in Fig. 6.7, provides the necessary current to achieve sufficient heating of the cathode. The designer of power tube amplifiers will always separate the DC resistance seen by the anode voltage supply from the AC resistance. This can be done by the use of a transformer, as shown in Fig. 6.7 or, for example, by implementing a large choke coil in parallel with the load resistor. Each remaining DC resistance will reduce the anode voltage and thereby increase the power that has to be delivered by the voltage supply to reach a given AC voltage amplitude on the load resistor. Usually, the input AC voltage to the control grid is also provided via a transformer, separating the AC generator (e.g., driver amplifier) from the DC control grid voltage. The input impedance of this transformer is usually matched to $50\ \Omega$ to allow the transmission of this input signal over a larger distance. According to the definition, the mutual conductance is given by

$$g_m = \left. \frac{\partial I_a}{\partial V_{g1}} \right|_{V_a}$$

⁴In most cases, the potential barrier introduced by the space charge effect of the high anode current alone is sufficient to inhibit the secondary electrons from traveling to the screen grid.

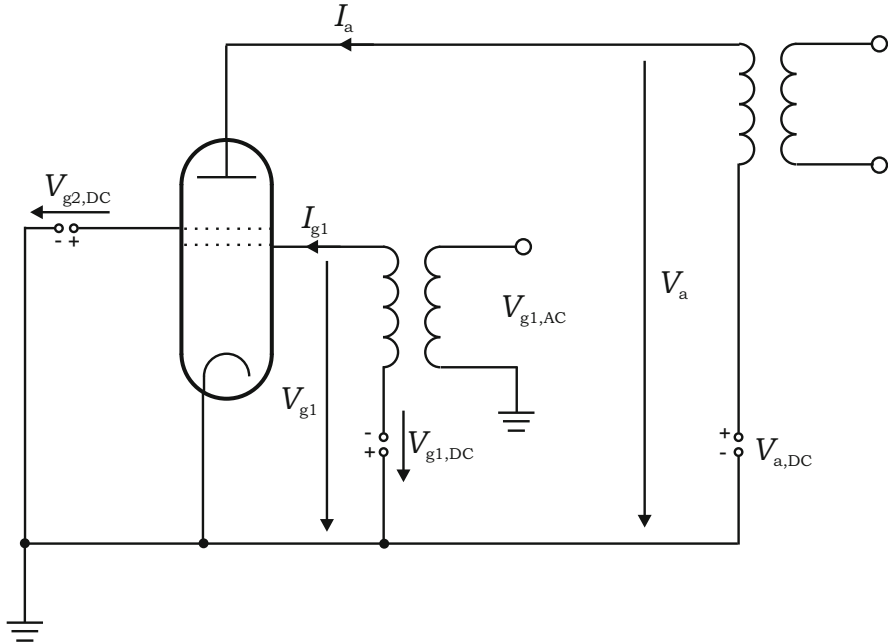


Fig. 6.7 Layout of a single-ended tube amplifier in grounded cathode configuration

for a sinusoidal control grid voltage

$$V_{g1,AC} = \hat{V}_{g1,AC} \cos(\omega t).$$

When using the orientations of voltages and currents as shown in Fig. 6.7, the anode AC current is given by

$$I_{a,AC} = g_m V_{g1,AC}.$$

This equation holds only in case of a short circuit operation. When R_a is larger than zero, the retroaction of the anode voltage on the anode current, moderated by the reverse amplification factor $1/\mu_a$, has to be taken into account (see Eq. (6.18)), resulting in

$$I_{a,AC} = g_m V_{ctrl,AC} \quad \text{with} \quad V_{ctrl,AC} = V_{g1,AC} + \frac{V_{a,AC}}{\mu_a}.$$

Using the Barkhausen equation (6.17),

$$\frac{g_m R_i}{\mu_a} = 1,$$

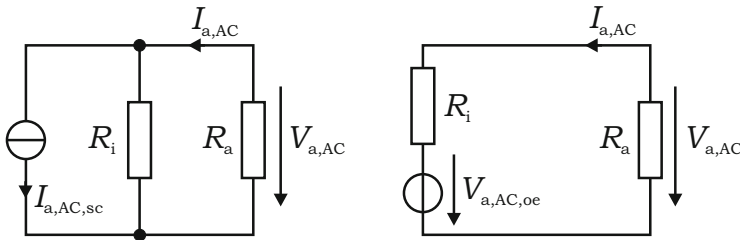


Fig. 6.8 Representation of a tube amplifier by a current source (*left*) or voltage source (*right*)

and $V_{a,AC} = -I_{a,AC}R_a$ leads to

$$I_{a,AC} = \frac{\mu_a V_{g1,AC}}{R_i + R_a},$$

$$V_{a,AC} = -\mu_a V_{g1,AC} \frac{R_a}{R_i + R_a}.$$

In case of a short circuit operation, this simplifies to

$$I_{a,AC,sc} = \frac{\mu_a V_{g1,AC}}{R_i},$$

$$V_{a,AC,sc} = 0,$$

and for open-ended operation, to

$$I_{a,AC,oe} = 0,$$

$$V_{a,AC,oe} = -\mu_a V_{g1,AC}.$$

The voltage amplification $\mu = -\hat{V}_{a,AC}/\hat{V}_{g1,AC}$ varies with the load resistance, remaining always below the open-ended amplification $\mu = \mu_a$.

The tube may be described as a current source or as a voltage source, as depicted in Fig. 6.8. These equivalent circuits describe the small-signal AC behavior of the tube as seen from the load. They cannot be used to describe the DC performance of the tube or the internal processes within the tube.

For each load resistance R_a , the relation between $V_{a,AC}$ and $I_{a,AC}$ is given by

$$V_{a,AC} = -R_a I_{a,AC}.$$

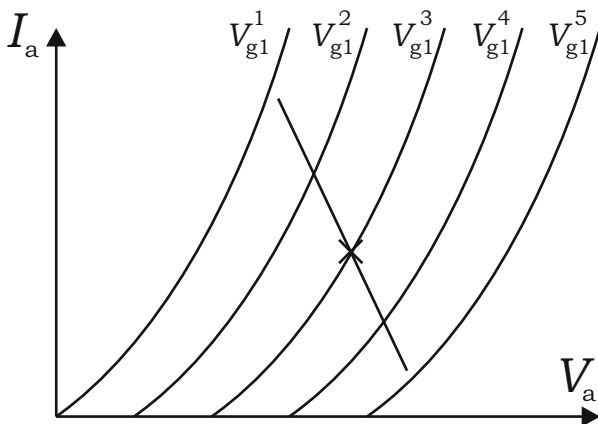


Fig. 6.9 Plate characteristics and example of a load line

The actual value of the anode current is given by

$$I_a = I_{a,DC} + I_{a,AC}$$

$$\Rightarrow I_a = I_{a,DC} - \frac{V_{a,AC}}{R_a}.$$

This represents the equation of a line with slope $-1/R_a$. The resulting line is called **load line** of the tube. An example of such a load line is shown in Fig. 6.9 together with exemplary plate characteristics of a tube. Such a diagram is a very efficient tool for visualizing the behavior of a tube amplifier under certain operational conditions. The line shows the actual values of the anode voltage, the anode current, and the control grid voltage for each moment in time. The point on the load line where $V_{g1} = V_{g1,DC}$ is called the **operating point** of the amplifier (cross in Fig. 6.9).

An amplifier can be used in different modes of operation, depending on the amount of time during which the amplifier provides current to the load. Here one distinguishes between class A, class B, and class C operation. The mode of operation is determined by the type of tube (the associated characteristic curves) and the choice of DC anode voltage, DC control grid voltage, AC control grid voltage, and screen grid voltage. Depending on these parameters, the tube may block the current flow for a certain period of one RF cycle.

If the parameters are chosen in such a way that the tube can provide current during the whole RF period, e.g., by keeping $V_{g1,DC}$ sufficiently high or $V_{g1,AC}$ sufficiently low for a given $V_{a,DC}$, the tube is used in **class A operation**. In class A operation, the anode current at the operating point differs only slightly from the DC anode current. The anode DC current is almost independent of the amplitude of the control grid AC voltage.

If the parameters ($V_{a,DC}$, $V_{g1,DC}$, $V_{g1,AC}$, $V_{g2,DC}$) are chosen in such a way that a given tube provides current for exactly half of each RF period, this is called

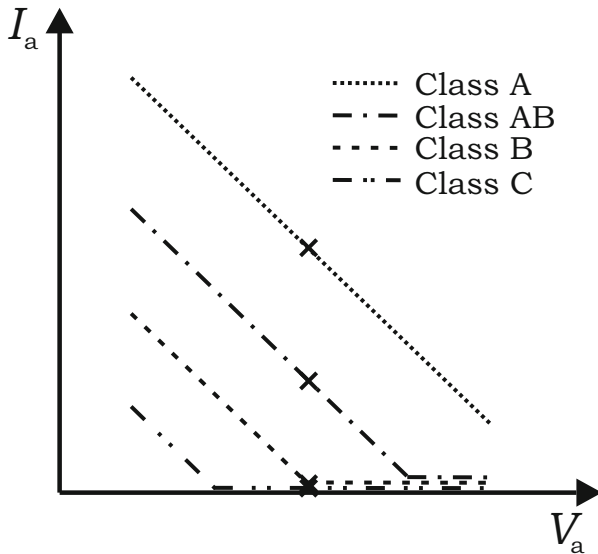


Fig. 6.10 Different classes of operation, typical operating lines of class A, AB, B, and C

class B operation. The anode current at the operating point is zero in an idealistic⁵ approximation, and the amplitude of the AC control grid voltage will have a strong influence on the DC anode current. All modes of operation between class A and class B are called **class AB** (e.g., if the tube delivers current for three-fourths of an RF period).

If the tube delivers current for less than half of an RF period, this operation is called **class C**. Again, the anode current at the operating point will be zero, and the amplitude of the control grid voltage will have an even stronger influence on the DC anode current. Idealized operating lines for different classes of operation are shown in Fig. 6.10. As will be discussed later, the efficiency of the amplifier as well as the amplitudes of the higher harmonic current components will increase when the class of operation changes from A to B to C.

One aim of amplifier development is to ensure that the output signal of the amplifier follows the input signal in a linear way. In the case of the amplifier discussed here, the actual value of the anode AC current has to be proportional to the actual value of the AC voltage at the control grid that will be delivered by a driver amplifier. There are several mechanisms that reduce this linearity. One reason for nonlinearities arises from positive control grid values. If the control grid is positive, a fraction of the current will begin to switch from the anode to the control grid. In addition, the activation of the control grid now requires input power during certain times of the period; this may induce further distortions of the

⁵Due to the characteristics of the tetrode, the anode current will not drop to zero sharply. It will be a continuous process.

control grid voltage. These imperfections can easily be avoided if the control grid is always operated at negative voltages. A second type of nonlinearity arises from a nonconstant amplification factor, which will have an impact on the anode current. If the anode voltage becomes sufficiently low compared to the screen grid voltage, a significant portion of the current emitted from the cathode may switch from the anode to the screen grid. Under these operating conditions, a slight variation of the anode voltage has a huge impact on the anode current; hence the amplification factor rises sharply in that region, producing nonlinearities. The extent of this type of distortion can be greatly reduced when the operating line of the tetrode is chosen in such a way that there is always a sufficient gap between the anode and the screen grid voltage. As mentioned earlier, the mutual conductance is not a constant; it varies strongly with the operating parameters of the tetrode, as can be seen here:

$$g_m = \left. \frac{\partial I_a}{\partial V_{g1}} \right|_{V_a}$$

Using Eq. (6.18) yields

$$g_m = \frac{3}{2} K_{\text{tetrode}} \sqrt{V_{g1} + \frac{V_a}{\mu_a} + \frac{V_{g2}}{\mu_{g2}}}$$

According to Eq. (6.18), this introduces a third type of nonlinearity that cannot be avoided. The amplitude of higher harmonic components of the anode current rises with the ratio between the AC anode and the DC anode current, as we will see now. Neglecting the influence of the anode voltage (short circuit operation), the anode current around the operating point can be expanded into a Taylor series

$$I_a = I_{a,\text{DC,op}} + A_1 V_{g1,\text{AC}} + \frac{1}{2} A_2 V_{g1,\text{AC}}^2 + \frac{1}{6} A_3 V_{g1,\text{AC}}^3 + \frac{1}{24} A_4 V_{g1,\text{AC}}^4 + \dots$$

with

$$A_1 = \left. \frac{dI_a}{dV_{g1}} \right|_{\text{op}}, \quad A_2 = \left. \frac{d^2 I_a}{dV_{g1}^2} \right|_{\text{op}}, \quad A_3 = \left. \frac{d^3 I_a}{dV_{g1}^3} \right|_{\text{op}}, \quad A_4 = \left. \frac{d^4 I_a}{dV_{g1}^4} \right|_{\text{op}}, \dots$$

Assuming a distortion-free signal

$$V_{g1,\text{AC}} = \hat{V}_{g1,\text{AC}} \cos(\omega t)$$

at the control grid results in

$$I_a = I_{a,\text{DC,op}} + A_1 \hat{V}_{g1,\text{AC}} \cos(\omega t) + \frac{1}{2} A_2 \hat{V}_{g1,\text{AC}}^2 \cos^2(\omega t) + \frac{1}{6} A_3 \hat{V}_{g1,\text{AC}}^3 \cos^3(\omega t) + \frac{1}{24} A_4 \hat{V}_{g1,\text{AC}}^4 \cos^4(\omega t) + \dots$$

Using

$$\cos^2(\omega t) = \frac{1}{2} + \frac{1}{2} \cos(2\omega t),$$

$$\cos^3(\omega t) = \frac{3}{4} \cos(\omega t) + \frac{1}{4} \cos(3\omega t),$$

$$\cos^4(\omega t) = \frac{3}{8} + \frac{1}{2} \cos(2\omega t) + \frac{1}{8} \cos(4\omega t),$$

yields

$$I_a = I_{a,DC,op} + \Delta I_a + \hat{I}_{a,AC,\omega} \cos(\omega t) + \hat{I}_{a,AC,2\omega} \cos(2\omega t) + \hat{I}_{a,AC,3\omega} \cos(3\omega t) + \dots$$

with

$$\Delta I_a = \frac{1}{4} A_2 \hat{V}_{g1,AC}^2 + \frac{1}{64} A_4 \hat{V}_{g1,AC}^4 + \dots, \quad (6.19)$$

$$\hat{I}_{a,AC,\omega} = A_1 \hat{V}_{g1,AC} + \frac{1}{8} A_3 \hat{V}_{g1,AC}^3 + \dots, \quad (6.20)$$

$$\hat{I}_{a,AC,2\omega} = \frac{1}{4} A_2 \hat{V}_{g1,AC}^2 + \frac{1}{48} A_4 \hat{V}_{g1,AC}^4 + \dots, \quad (6.21)$$

$$\hat{I}_{a,AC,3\omega} = \frac{1}{24} A_3 \hat{V}_{g1,AC}^3 + \dots. \quad (6.22)$$

The quantity ΔI_a represents the shift of the DC anode current with respect to the anode current at the operating point due to the asymmetric characteristic current curves. As mentioned during the discussion of the different classes of amplifier operation, this shift increases with rising amplitude of the control grid voltage and especially in moving from class A to class B or class C. The quantity $\hat{I}_{a,AC,n\omega}$ describes the amplitude of the n th fundamental of the anode current. Again, the higher harmonic content rises when the amplitude of the control grid voltage increases as well as in moving from class A to class B or class C operation.

In order to quantify the harmonic distortion, we will use the ratio

$$k_{hd,n} = \frac{\hat{I}_{a,AC,n\omega}}{\hat{I}_{a,AC,\omega}}.$$

for the individual harmonics.

We will now perform a first estimation regarding the amount of harmonic distortion for a particular mode of operation of a tube. Note that these approximations

assume that the tube is operated in the space-charge-limited region, which is strictly true only in class A operation. Furthermore, for the sake of simplicity, the effect of a variation of the anode voltage on the anode current is again neglected (short-circuit approximation).

In the space-charge-limited region, we have

$$I_a = K_{\text{tetrode}} V_{\text{ctrl}}^\zeta = K_{\text{tetrode}} \left(V_{g1} + \frac{V_{g2}}{\mu_{g2}} + \frac{V_a}{\mu_a} \right)^\zeta.$$

This equation is based on Eq. (6.18), but we now assume a general exponent ζ instead of the specific value $3/2$, since this may be useful in describing specific tubes more accurately.

For the operating point,

$$I_{a,\text{DC,op}} = K_{\text{tetrode}} V_{\text{ctrl,DC,op}}^\zeta$$

is valid, so that

$$A_1 = \left. \frac{dI_a}{dV_{g1}} \right|_{\text{op}} = \zeta K_{\text{tetrode}} V_{\text{ctrl,DC,op}}^{\zeta-1} = \zeta \frac{I_{a,\text{DC,op}}}{V_{\text{ctrl,DC,op}}}$$

$$A_2 = \left. \frac{d^2 I_a}{dV_{g1}^2} \right|_{\text{op}} = \zeta(\zeta - 1) K_{\text{tetrode}} V_{\text{ctrl,DC,op}}^{\zeta-2} = \zeta(\zeta - 1) \frac{I_{a,\text{DC,op}}}{V_{\text{ctrl,DC,op}}^2}$$

is obtained. Equation (6.20) leads to

$$\hat{I}_{a,\text{AC},\omega} \approx A_1 \hat{V}_{g1,\text{AC}} = \zeta I_{a,\text{DC,op}} \frac{\hat{V}_{g1,\text{AC}}}{V_{\text{ctrl,DC,op}}}. \quad (6.23)$$

Equation (6.19) yields

$$\Delta I_a \approx \frac{1}{4} A_2 \hat{V}_{g1,\text{AC}}^2 = \frac{1}{4} \zeta(\zeta - 1) I_{a,\text{DC,op}} \frac{\hat{V}_{g1,\text{AC}}^2}{V_{\text{ctrl,DC,op}}^2}.$$

By means of Eq. (6.23), this may be written as

$$\Delta I_a \approx \frac{1}{4} \frac{\zeta - 1}{\zeta} \frac{\hat{I}_{a,\text{AC},\omega}^2}{I_{a,\text{DC,op}}}.$$

Equation (6.21) leads to

$$\hat{I}_{a,\text{AC},2\omega} \approx \frac{1}{4} A_2 \hat{V}_{g1,\text{AC}}^2 = \frac{1}{4} \zeta(\zeta - 1) I_{a,\text{DC,op}} \frac{\hat{V}_{g1,\text{AC}}^2}{V_{\text{ctrl,DC,op}}^2}. \quad (6.24)$$

By means of Eq. (6.23), this may be written as

$$\hat{I}_{a,AC,2\omega} \approx \frac{1}{4} \frac{\zeta - 1}{\zeta} \frac{\hat{I}_{a,AC,\omega}^2}{I_{a,DC,op}}.$$

This allows us to calculate

$$k_{hd,2} = \frac{\hat{I}_{a,AC,2\omega}}{\hat{I}_{a,AC,\omega}} \approx \frac{1}{4} \frac{\zeta - 1}{\zeta} \frac{\hat{I}_{a,AC,\omega}}{I_{a,DC,op}}. \quad (6.25)$$

It can be seen that in this approximation, the second harmonic distortion increases proportionally to the ratio of the amplitude of the current of the fundamental harmonic compared to the current of the operating point. So these distortions can be reduced either by reducing the AC current or by increasing the current at the operating point.

By means of Eq. (6.23), the result (6.25) may alternatively be written as

$$k_{hd,2} = \frac{\hat{I}_{a,AC,2\omega}}{\hat{I}_{a,AC,\omega}} \approx \frac{1}{4} (\zeta - 1) \frac{\hat{V}_{g1,AC}}{V_{ctrl,DC,op}}.$$

The efficiency of the class A power amplifier may be defined by the ratio between the RF power at the fundamental harmonic (only this is useful for standard acceleration) delivered to the cavity and the DC power received by the amplifier:

$$\eta_{ampl} = \frac{P_{a,AC,\omega}}{P_{a,DC,op}}.$$

With

$$P_{a,AC,\omega} = \frac{1}{2} \hat{V}_{a,AC,\omega} \hat{I}_{a,AC,\omega}$$

and

$$P_{a,DC,op} = V_{a,DC,op} I_{a,DC,op},$$

we obtain

$$\eta_{ampl} = \frac{1}{2} \frac{\hat{V}_{a,AC,\omega} \hat{I}_{a,AC,\omega}}{V_{a,DC,op} I_{a,DC,op}}.$$

Here one can see that the efficiency is proportional to the ratio of the amplitude of the current of the fundamental harmonic to the DC current of the operating point. This emphasizes that system efficiency and minimal distortion are contradicting targets in the design of a synchrotron RF amplifier. In general, the ratio $\hat{I}_{a,AC,\omega}/I_{a,DC,op}$ cannot

exceed 1 in class A operation, and the ratio $\hat{V}_{a,AC,\omega} / V_{a,DC,op}$ always stays below 1, due to the fact that the anode voltage always has to remain sufficiently above the screen grid voltage to ensure that (electron) current can flow from the cathode to the anode. Therefore, the efficiency in class A operation is limited to

$$\eta_{\text{ampl}} < \frac{1}{2}.$$

6.3 Tube Operation

The power delivered by the tetrodes used for synchrotron cavities is rather high, and these tubes are operated at moderate efficiencies, resulting in a significant heat load of the tetrodes. Most synchrotron cavity power amplifiers are designed in such a way that they can also be operated without RF input for some time. In that case, the efficiency is zero, and the whole power delivered by the power supplies is dissipated in the tube. This power has to be removed by active cooling systems to prevent overheating of the tetrode, which would result in melting and the destruction of the tube. Usually two different methods of cooling are applied: Most of the power is dissipated in the anode of the tetrode, which is cooled effectively by deionized water. The water requirements such as conductivity, flow rate, and pressure drop are usually listed in the data sheet of the tube. The remaining heat load (e.g., grid, cathode) is handled by forced air cooling of the tube casing and socket.

The tubes must be handled with care to maximize the lifetime. This includes certain precautions in transporting or handling the tube. It is, for example, very important to restrict the maximum acceleration force experienced by the tube. Certain operating parameters of the tetrode, e.g., anode or grid voltages and currents, must not exceed predefined values. These values have to be observed during operation, and appropriate action, e.g., a normal or a fast shutdown procedure, has to be taken when one of these values exceeds its threshold. In some cases, especially in case of an overcurrent on the grids, this shutdown procedure has to be performed very fast. Therefore, the crucial parameters have to be monitored by a fast electronic module, and the reacting device—usually located in the power supply unit—that is responsible for the grounding of tetrode voltages also has to be fast (e.g., ignitron or solid state switch). In case of a pulsed RF system that uses tetrodes above their CW rating, it is also necessary to monitor the total amount of power dissipated in the tetrode during each pulse. This can be done by integrating the DC power delivered to the tetrode and the RF power provided by it. When the difference between these two quantities exceeds a predefined threshold, the tube has to be shut down.

Special care has to be taken regarding the activation and deactivation of the tetrode. The sequence used to activate and deactivate the different power supplies is crucial. Regarding activation, first the cathode supply (filament) is turned on. It may take up to several minutes for the cathode to reach a stable temperature;

afterward, the negative DC voltage of the control grid is applied before the main anode voltage is turned on. Finally, the screen grid voltage is activated. Now the tube is ready to operate. This sequence ensures that there will be no excessive current from the cathode to one of the grids or toward the anode. This sequence is reversed in deactivating the tube.

References

1. K.R. Spangenberg, *Vacuum Tubes* (McGraw-Hill, New York/Toronto/London, 1948)
2. R.G. Carter, RF power generation, in *CAS - CERN Accelerator School: RF for Accelerators*, Ebeltoft, 8–17 Jun 2010, pp. 173–207
3. H. Barkhausen, E.-G. Woschni, *Lehrbuch der Elektronenröhren*, Band 1, 12. Auflage (S. Hirzel Verlag, Leipzig, 1969)
4. A.H.W. Beck, *Thermionic Valves: Their Theory and Design* (Cambridge University Press, Cambridge, 1953)
5. D. Preist, M. Shrader, The klystrode — an unusual transmitting tube with potential for UHF-TV. *Proc. IEEE* **70**(11), 1318–1325 (1982)
6. A.S. Gilmour, *Klystrons, Traveling Wave Tubes, Magnetrons, Crossed-Field Amplifiers, and Gyrotrons* (Artech House, Norwood, 2011)
7. I. Langmuir, The effect of space charge and initial velocities on the potential distribution and thermionic current between parallel plane electrodes. *Phys. Rev.* **21**, 419–435 (1923)
8. X. Chen, J. Dickens, L.L. Hatfield, E.-H. Choi, M. Kristiansen, Approximate analytical solutions for the space-charge-limited current in one-dimensional and two-dimensional cylindrical diodes. *Phys. Plasmas* **11** (2004) <http://dx.doi.org/10.1063/1.1743309>
9. H. Barkhausen, E.-G. Woschni, *Lehrbuch der Elektronenröhren*, Band 2, 10. Auflage (S. Hirzel Verlag, Leipzig, 1968)



This chapter is licensed under the terms of the Creative Commons Attribution-NonCommercial-NoDerivatives 4.0 International License (<https://creativecommons.org/licenses/by-nc-nd/4.0/>), which permits any noncommercial use, sharing, distribution and reproduction in any medium or format, as long as you give appropriate credit to the original author(s) and the source, provide a link to the Creative Commons license and indicate if you modified the licensed material. You do not have permission under this license to share adapted material derived from this chapter or parts of it.

The images or other third party material in this chapter are included in the chapter's Creative Commons license, unless indicated otherwise in a credit line to the material. If material is not included in the chapter's Creative Commons license and your intended use is not permitted by statutory regulation or exceeds the permitted use, you will need to obtain permission directly from the copyright holder.